GEOPHYSICAL RESEARCH LETTERS

Supporting Information for

Contributions of World Regions to the Global Tropospheric Ozone Burden Change from 1980 to 2010

Yuqiang Zhang[1], J. Jason West[2], Louisa Emmons[3], Johannes Flemming[4,] Jan Eiof Jonson[5], Marianne Tronstad Lund[6], Takashi Sekiya[7], Kengo Sudo[7]

[1]Nicholas School of the Environment, Duke University, 9 Circuit Dr, Durham, NC 27708, USA.

[2]Environmental Sciences and Engineering Department, University of North Carolina at Chapel Hill, Chapel Hill, North Carolina 27599, USA.

[3]Atmospheric Chemistry Observations and Modeling Laboratory, National Center for Atmospheric Research (NCAR), Boulder, CO, USA

[4]European Center for Medium-Range Weather Forecasts, Reading, UK

[5]Norwegian Meteorological Institute, Oslo, Norway

[6]CICERO Center for International Climate Research, Oslo, Norway

[7]Japan Agency for Marine-Earth Science and Technology, Yokohama, Japan

[8]Nagoya University, Furocho, Chigusa-ku, Nagoya, Japan

Contents of this file

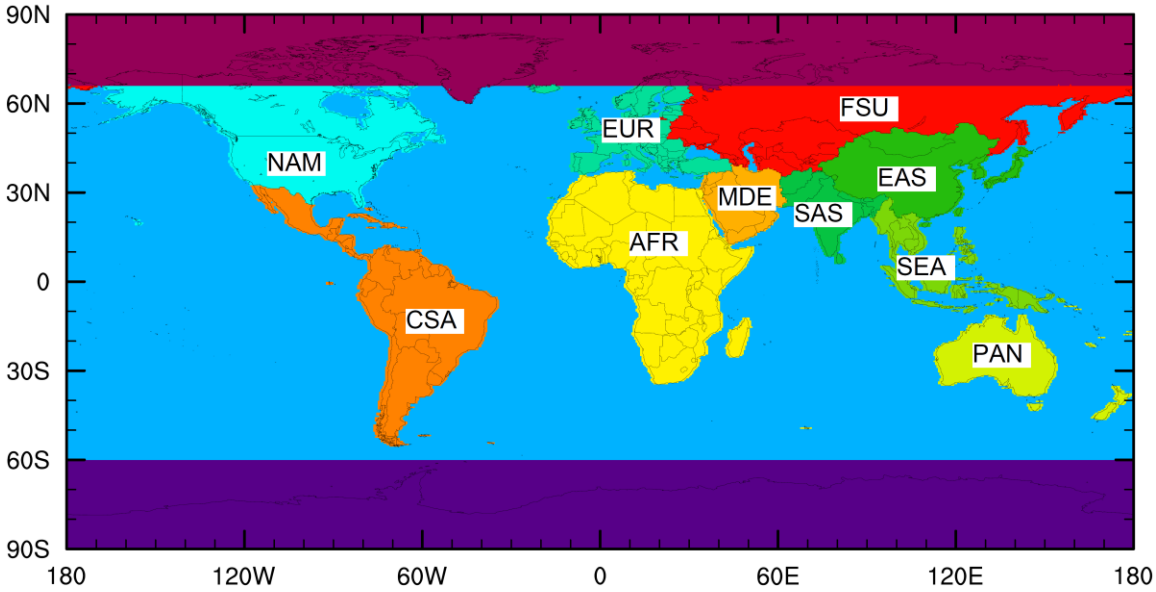

Figure S1. The 10 world regions definitions, including two extra grid cells along the coastal regions. Most of the regions are following the HTAP2 definitions (http://iek8wikis.iek.fz-juelich.de/HTAPWiki/WP2.1, last access July 2 2018), such as North America (NAM, including USA and Canada), Europe (EUR), South Asia (SAS), East Asia (EAS), South East Asia (SEA), Pacific, Australia and New Zealand (PAN), Middle East (MDE). We group Northern Africa and Sub Saharan together as new region Africa (AFR). We then group Mexico and Central America and South America together as region Central South America (CSA). We group Russia, Belarussia, Ukraine and Central Asia as region Former Soviet Union (FSU). Blue color means the Ocean region (OCN). Dark red means Arctic Circle (North of 66 N) + Greenland (NPO). Purple color means Antarctic (SPO).

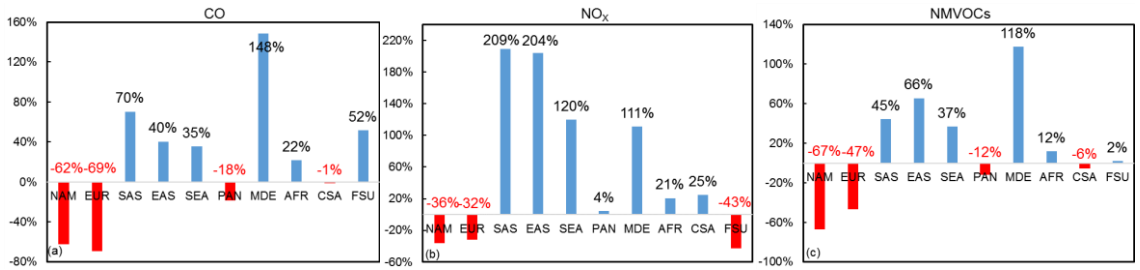

Figure S2: Percent emission changes for CO (a, (2010-1980)/1980×100%), NO_x (b), and NMVOCs (c) from 1980 to 2010 for the 10 world regions. The red color shows regions with emission decreases, and blue color shows emission increases.

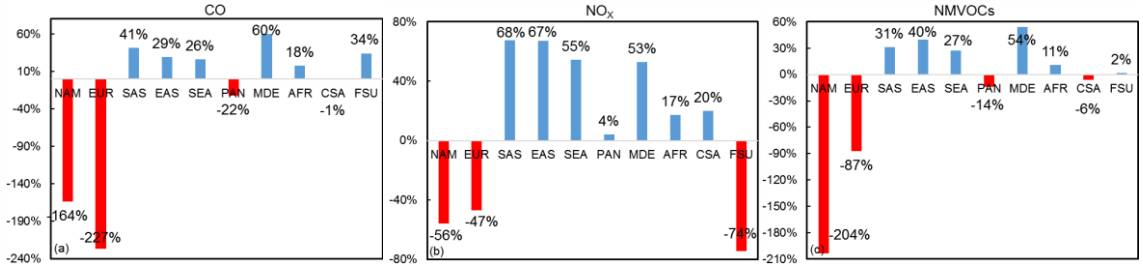

Figure S3. As for Fig. S2, but the differences are calculated as relative to the emissions totals in 2010 ((2010-1980)/2010×100%).

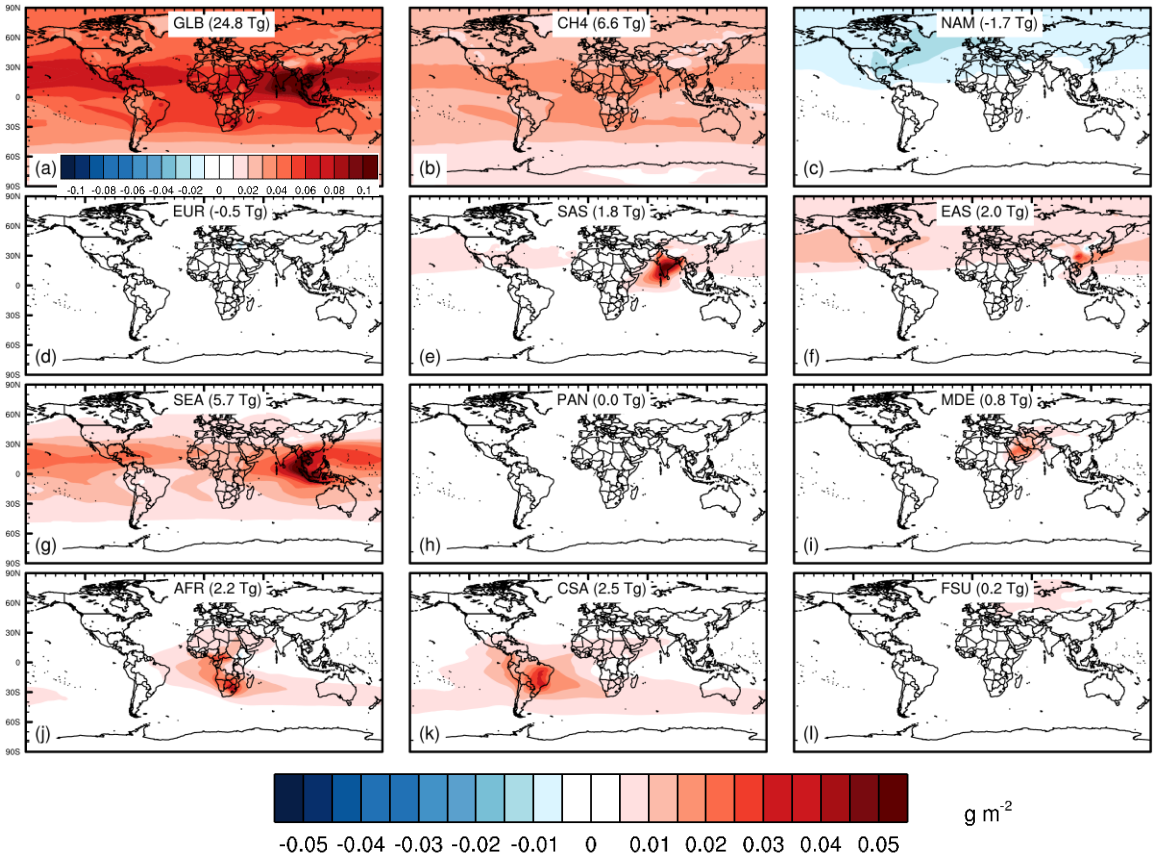

Figure S4: Spatial distributions of ΔBO_3 (g m^{-2}) from 1980 to 2010 for the season DJF, for (a) total emission changes from 1980 to 2010, (b) global CH_4 concentration change, and (c)-(l) emission changes in 10 world regions.

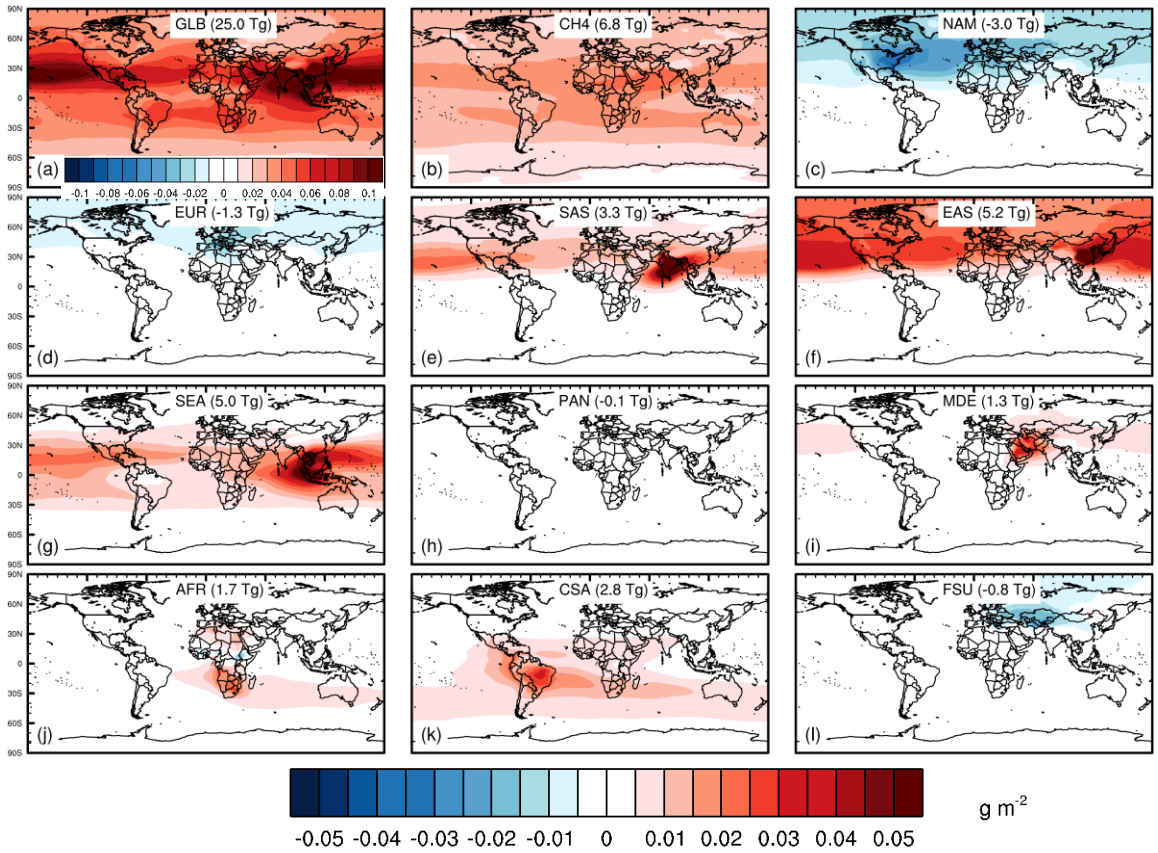

Figure S5: As in Fig. S4 but for MAM.

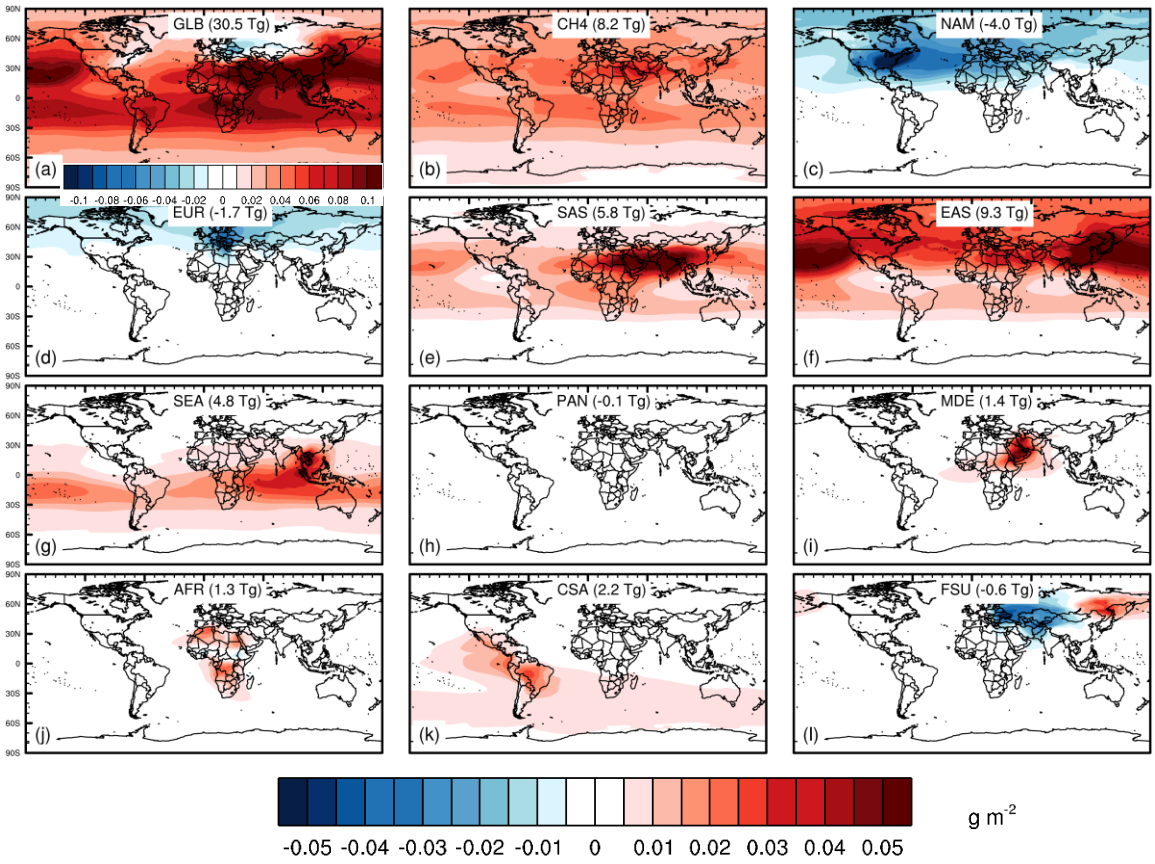

Figure S6: As in Fig. S4 but for JJA.

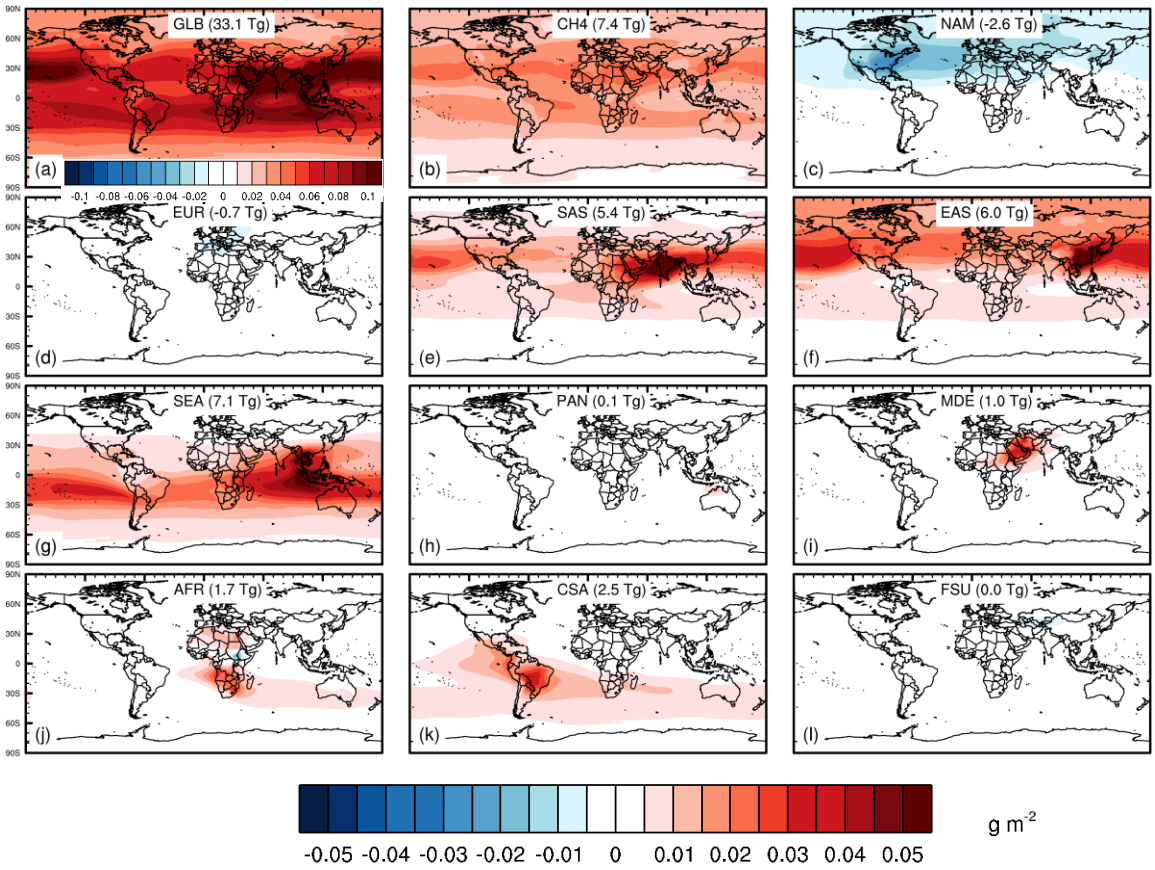

Figure S7: As in Fig. S4 but for SON.

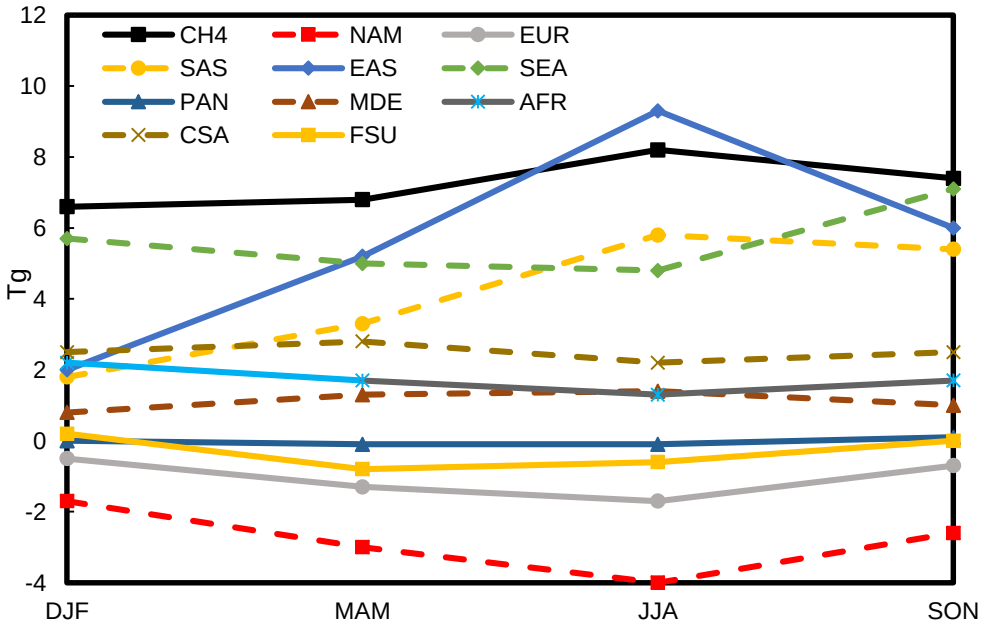

Figure S8: Seasonal distributions of the global tropospheric ozone burden changes between 1980 and 2010 from changes in the global CH_4 concentration, and regional emissions.

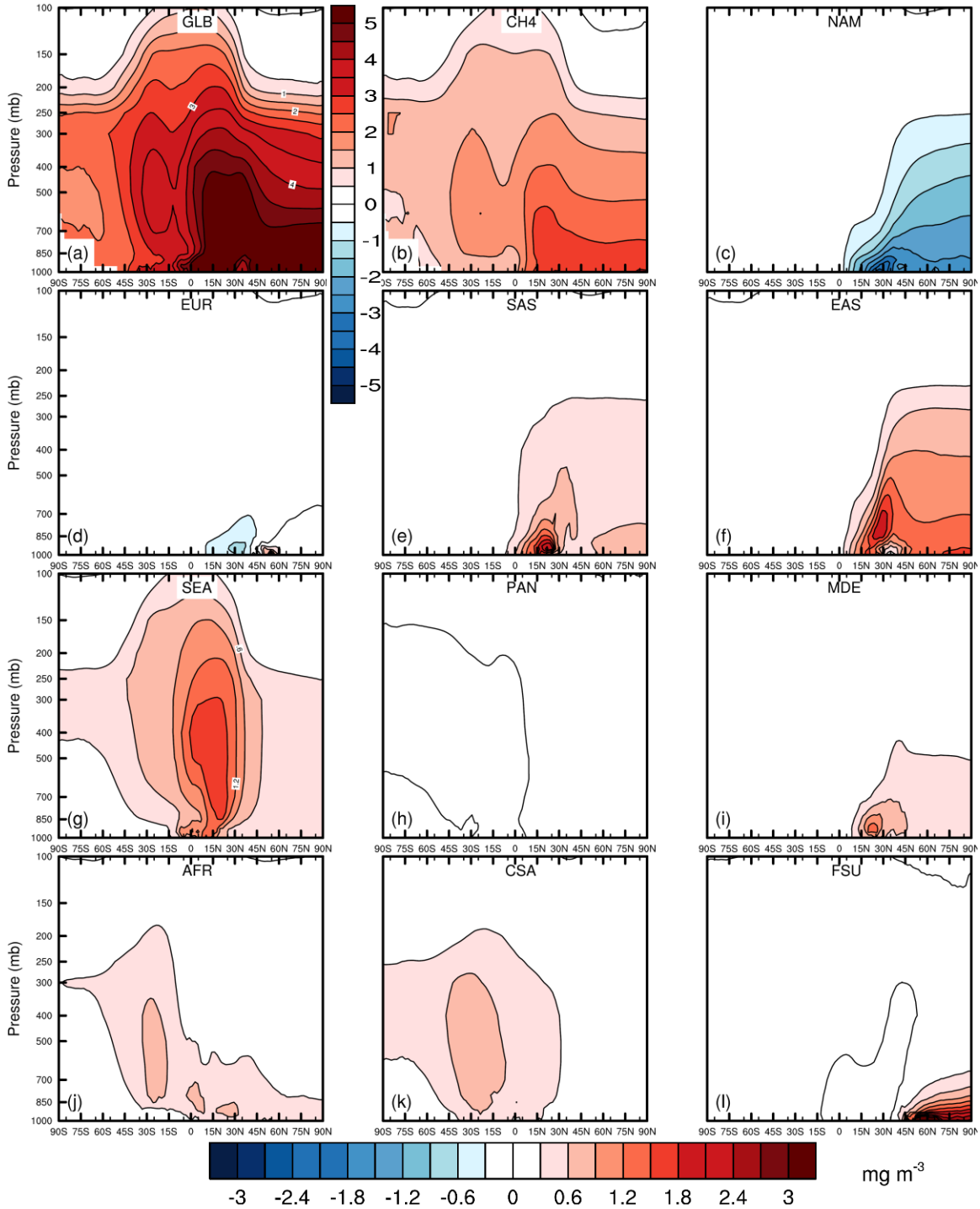

Figure S9: Zonal DJF mean O_3 change (mg m^{-3}) from 1980 to 2010, for (a) total emission changes from 1980 to 2010, (b) global CH_4 concentration change, and (c)-(l) emission changes in 10 world regions.

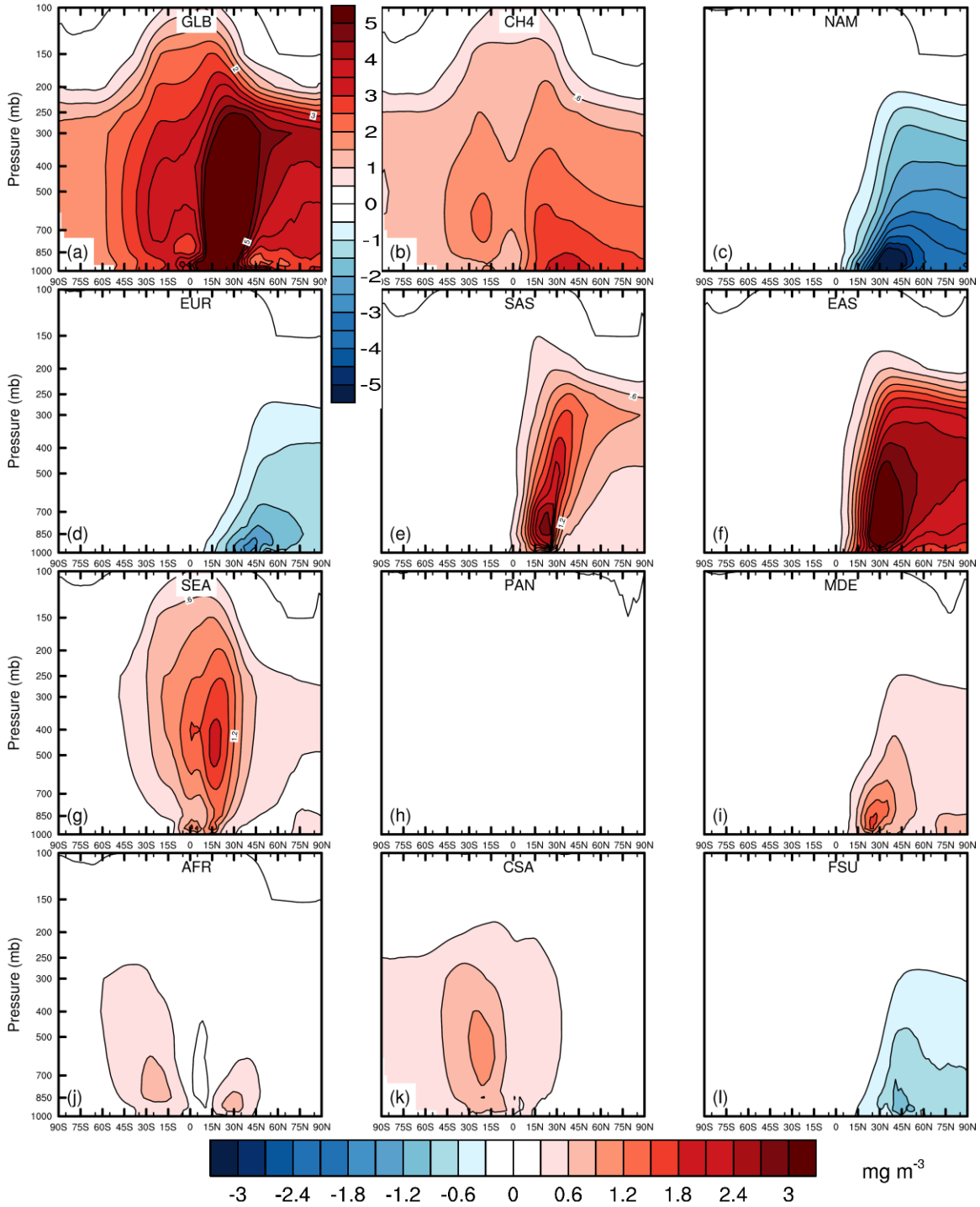

Figure S10: As in Fig. S9 but for MAM**.**

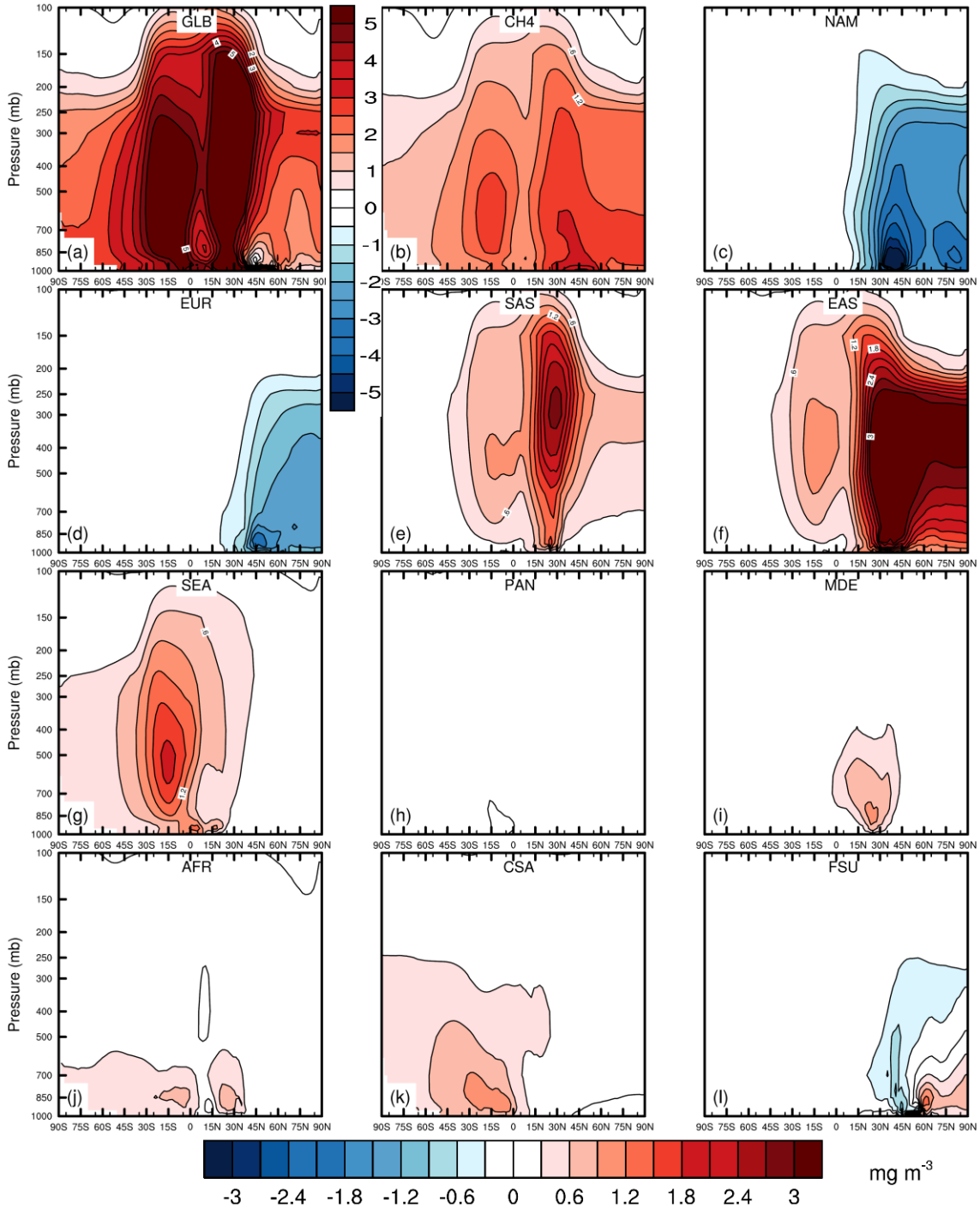

Figure S11: As in Fig. S9 but for JJA.

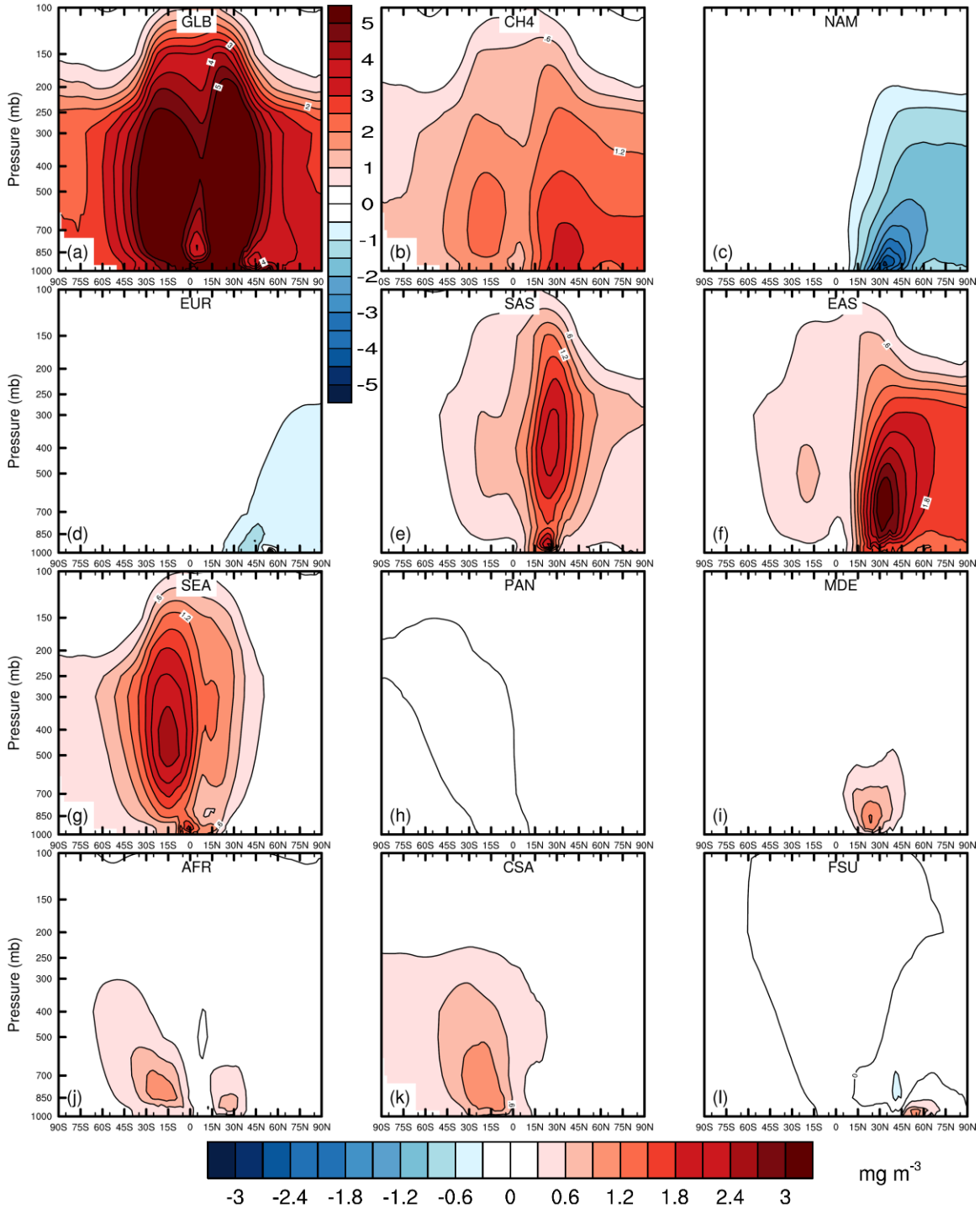
GLB
CH4
NAM
EUR
SAS
EAS
SEA
PAN
MDE
AFR
CSA
FSU
(a)
(b)
(c)
(d)
(e)
(f)
(g)
(h)
(i)
(j)
(k)
(l)
Pressure (mb)
100
150
200
250
300
400
500
700
850
1000
90S 75S 60S 45S 30S 15S 0 15N 30N 45N 60N 75N 90N
5
4
3
2
1
0
-1
-2
-3
-4
-5
-3 -2.4 -1.8 -1.2 -0.6 0 0.6 1.2 1.8 2.4 3
mg m-3

Figure S12: As in Fig. S9 but for SON.

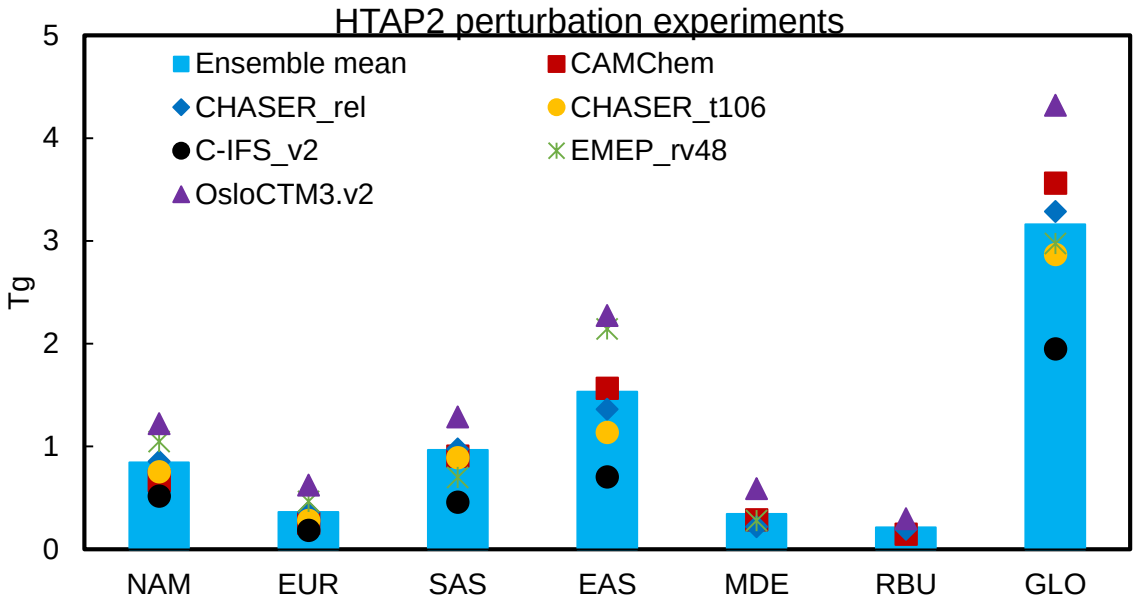

Figure S13: Global tropospheric ozone burden changes between the base and 7 perturbation experiments. The blue columns are the ensemble model mean from the 6 available models. Note that both the CHASER_t106 and C-IFS_v2 did not perform the MDE and RBU perturbation experiments, and the EMEP_rv48 model did not perform the RBU experiment. The global ozone burden changes for GLO experiments are divided by 3 for all the single and ensemble models to better fit the plot.

Table S1. Model simulations discussed in this study. The first three simulations (S_2010, S_1980, and S_CH_4) were performed in our last study (Zhang et al., 2016). The global methane concentration has increased from 1567 ppbv in 1980 to 1798 ppbv in 2010 (Prather et al., 2013).

	Anthropogenic and Biomass burning emissions in year	Global CH_4 concentration
S_2010	2010	1798 ppbv
S_1980	1980	1567 ppbv
S_CH_4	2010	1567 ppbv
S_NAM	2010 worldwide, 1980 in North America	1798 ppbv
S_EUR	2010 worldwide, 1980 in except for Europe	1798 ppbv
S_SAS	2010 worldwide, 1980 in South Asia	1798 ppbv
S_EAS	2010 worldwide, 1980 in East Asia	1798 ppbv
S_SEA	2010 worldwide, 1980 in South East Asia	1798 ppbv
S_PAN	2010 worldwide, 1980 in Pacific, Australia and New Zealand	1798 ppbv
S_MDE	2010 worldwide, 1980 in for Middle East	1798 ppbv
S_AFR	2010 worldwide, 1980 in Africa	1798 ppbv
S_CSA	2010 worldwide, 1980 in Central South America	1798 ppbv
S_FSU	2010 worldwide, 1980 in Former Soviet Union	1798 ppbv

Table S2. Regional anthropogenic emissions in 1980 and 2010 for CO, including biomass burning, and the differences in regional emissions from adding two extra grid cells. Units are Tg CO yr^{-1}. The 10 regions are defined in Figure S1.

	With 2 extra coastal grid cells			**Differences between with and without 2 extra grid cells**	
	1980	2010	Diff (Relative)	1980	2010
NAM	139.2	52.7	-86.5 (-62%)	6.0	2.0
EUR	87.4	26.8	-60.6 (-69%)	9.0	2.8
SAS	65.2	111.1	45.9 (70%)	4.0	6.6
EAS	116.2	163.2	47.0 (40%)	9.5	10.4
SEA	91.3	123.6	32.3 (35%)	18.0	24.0
PAN	25.8	21.1	-4.7 (-18%)	2.6	2.1
MDE	8.6	21.5	12.8 (148%)	0.7	1.9
AFR	228.8	278.6	49.9 (22%)	4.2	6.6
CSA	106.8	105.5	-1.2 (-1%)	5.2	5.2
FSU	42.4	64.3	21.9 (52%)	0.8	1.6
Sum[1]	911.8	968.4	56.7 (6%)	60.0	63.2
Global[2]	**967.8**	**1029.9**	**62.1 (6.4%)**		

[1]Sum are the emission totals from the 10 inland regions.

[2]Global are the emission total in all the grid cells. The differences between the Global and the Sum are the emissions over the ocean, NPO and SPO (see Figure S1).

Table S3. The same as Table S2, but for NO_x. Units are Tg NO_x yr^{-1}.

	W/ extra 2 coastal grid cells			Differences between w/ and w/o extra 2 grid cells	
	1980	2010	Diff (Relative)	1980	2010
NAM	21.2	13.6	-7.6 (-36%)	1.2	0.8
EUR	15.2	10.3	-4.8 (-32%)	1.8	1.5
SAS	2.6	8.0	5.4 (209%)	0.2	0.5
EAS	8.1	24.7	16.6 (204%)	1.1	2.1
SEA	2.5	5.5	3.0 (120%)	0.6	1.3
PAN	2.1	2.2	0.1 (4%)	0.3	0.3
MDE	2.1	4.4	2.3 (111%)	0.2	0.5
AFR	13.1	15.8	2.7 (21%)	0.4	0.7
CSA	7.1	8.8	1.8 (25%)	0.7	0.8
FSU	13.7	7.8	-5.8 (-43%)	0.3	0.2
Sum[1]	87.6	101.2	13.6 (15%)	6.9	8.6
Global[2]	**104.0**	**126.1**	**22.1 (21.2%)**		

Table S4. The same as Table S2, but for NMVOCs. Units are Tg NMVOCs yr^{-1}.

	W/ extra 2 coastal grid cells			Differences between w/ and w/o extra 2 grid cells	
	1980	2010	Diff (Relative)	1.6	0.5
NAM	24.9	8.2	-16.7 (-67%)	1.5	0.9
EUR	13.6	7.3	-6.4 (-47%)	0.4	0.6
SAS	8.3	12.0	3.7 (45%)	1.4	2.0
EAS	16.3	26.9	10.7 (66%)	3.4	4.7
SEA	16.0	22.0	6.0 (37%)	0.4	0.4
PAN	3.6	3.2	-0.4 (-12%)	0.8	1.7
MDE	6.6	14.3	7.7 (118%)	0.8	1.2
AFR	35.6	39.9	4.3 (12%)	1.4	1.3
CSA	21.3	20.1	-1.2 (-6%)	0.2	0.3
FSU	11.4	11.6	0.2 (2%)	12.1	13.6
Sum[1]	157.7	165.5	7.8 (5%)	1.6	0.5
Global[2]	**170.1**	**180.3**	**10.2 (6.0%)**		

Table S5. Available models that simulate the 20% emission perturbation experiments in global and 6 Tier 1 source regions from HTAP2, with reporting hourly O_3 at different model levels. Data are available upon request from http://aerocom.met.no, last accessed Feb 28, 2019.

Models	Institution	Contact	Model resolution (lon×lat)	Reference
CAMchem	NCAR	Louisa Emmons	2.5° × 1.9°	Tilmes et al., 2016
CHASER_rel	NAGOYA, JAMSTEC, NIES	Kengo Sudo Takashi Sekiya	2.8° × 2.8°	Sudo et al., 2002
CHASER_t106	As above	As above	1.1° × 1.1°	Sudo et al., 2002
C-IFS_v2	ECMWF	Johannes Flemming	0.7° × 0.7°	Flemming et al., 2015
EMEP_rv48	Met No	Jan Eiof Jonson	0.5° × 0.5°	Simpson et al., 2012
OsloCTM3.v2	CICERO	Marianne Tronstad Lund	2.8° × 2.8°	Søvde et al., 2012

References:

Flemming, J., Huijnen, V., Arteta, J., Bechtold, P., Beljaars, A., Blechschmidt, A.-M., et al. (2015). Tropospheric chemistry in the Integrated Forecasting System of ECMWF, Geosci. Model Dev., 8, 975–1003, https://doi.org/10.5194/gmd-8-975-2015.

Sudo, K., Takahashi, M., Kurokawa, J.-I., and Akimoto, H. (2002). CHASER: A global chemical model of the troposphere 1. Model description, J. Geophys. Res.-Atmos., 107, ACH 7-1–ACH 7-20. https://doi.org/10.1029/2001JD001113.

Tilmes, S., Lamarque, J. F., Emmons, L. K., Kinnison, D. E., Marsh, D., Garcia, R. R., et al. (2016). Representation of the Community Earth System Model (CESM1) CAM4-chem within the Chemistry-Climate Model Initiative (CCMI). *Geoscientific Model Development*, *9*(5), 1853–1890. https://doi.org/10.5194/gmd-9-1853-2016

Simpson, D., Benedictow, A., Berge, H., Bergström, R., Emberson, L. D., Fagerli, H., et al. (2012). The EMEP MSC-W chemical transport model – technical description, Atmos. Chem. Phys., 12, 7825–7865, https://doi.org/10.5194/acp-12-7825-2012.

Søvde, O. A., Prather, M. J., Isaksen, I. S. A., Berntsen, T. K., Stordal, F., Zhu, X., et al. (2012). The chemical transport model Oslo CTM3, Geosci. Model Dev., 5, 1441–1469, https://doi.org/10.5194/gmd-5-1441-2012.